Short communication

Improvement of the high rate capability of hierarchical structured $Li_4Ti_5O_{12}$ induced by the pseudocapacitive effect

C. Lai, Y.Y. Dou, X. Li, X.P. Gao*

Institute of New Energy Material Chemistry, Tianjin Key Laboratory of Metal and Molecule Based Material Chemistry, Nankai University, Tianjin 300071, China

ABSTRACT

Hierarchical structured $Li_4Ti_5O_{12}$, assembling from randomly oriented nanosheets with a thickness of about 10–16 nm, is fabricated by a facile hydrothermal route and following calcination. It is demonstrated that the as-prepared sample has good cycle stability and excellent high rate performance. In particular, the discharge capacity of 128 mAh g^{-1} can be obtained at the high current density of 2000 mA g^{-1}, which is about 87% of that at the low current density of 200 mA g^{-1} upon cycling, indicating that the as-prepared sample can endure great changes of various discharge current densities to retain a good stability. In addition, the pseudocapacitive effect based on the hierarchical structure, also contributes to the high rate capability of $Li_4Ti_5O_{12}$, which can be confirmed in cyclic voltammograms.

© 2009 Elsevier B.V. All rights reserved.

1. Introduction

Safety is one of the primary concerns in the applications of lithium-ion batteries, especially for automobile applications [1,2]. Among those safe alternatives for graphite anode, $Li_4Ti_5O_{12}$ is of particular interest due to its extreme flat operation potential plateau at about 1.5 V vs. Li$^+$/Li to avoid the deposition of metallic lithium and negligible structural change during the discharge/charge process to ensure superior cycle stability [3]. However, the inherent insulating character of $Li_4Ti_5O_{12}$ seriously limits its high rate capability, a key parameter to obtain the high power density of batteries [3–10]. To improve the high rate capability of $Li_4Ti_5O_{12}$, many attempts have been made in the past, such as introducing conductive additives and fabricating nanostructured $Li_4Ti_5O_{12}$ [3–10]. Here nanostructured $Li_4Ti_5O_{12}$ can serve to shorten the diffuse distance of lithium ion and electron, and increase contact area between electrode and electrolyte, thus improving its high rate capability [3,5,10,11]. Moreover, reducing the grain size into nanoscale can offer some further exciting features, for example, the pseudocapacitive effect existing in nanostructured TiO_2 and titanate [12–16]. The faradaic pseudocapacitive characteristic is mainly related to surface charge-transfer process, which can provide extra charge storage and faster charge/discharge rate [15,16].

In this work, we have prepared micro-sized $Li_4Ti_5O_{12}$ particles consisting with nanosheets via a facile hydrothermal route, which is an attractive architecture for the Li-ion battery electrode. The nanosheets are possible to present a pseudocapacitive effect as the interaction taking place on the surface, thus leading to improved high rate capability [14]. The particle size in the micrometer range can increase the volume energy densities compared to low-dimensional nanomaterials [11]. Furthermore, the hierarchical structured $Li_4Ti_5O_{12}$ can share the same advantages as nanostructured electrode materials as mentioned above. Thus, the as-prepared sample can be expected to present an excellent electrochemical performance as confirmed by the electrochemical tests of the galvanostatic method and cyclic voltammetry.

2. Experimental

2.1. Preparation and characterization

Precursor solution as titanium source is prepared by dissolving 6.26 g $TiOSO_4\cdot2H_2O$ (Chemical) in 80 ml H_2O. The as-prepared $TiOSO_4$ solution (5 ml) is mixed with 15 ml H_2O, and then adding dropwise into 20 ml solution that contains 0.336 g $LiOH\cdot H_2O$ (analytical) and 0.1 g urea (analytical). After stirring for 3 min, the resultant solution is transferred into a Teflon-lined autoclave (55 ml) and treated at 180 °C for 24 h. The obtained precipitates were washed with original solution and about 12 ml ethanol for one time, respectively. The way of washing is key to obtain pure $Li_4Ti_5O_{12}$. After dried at 80 °C for 24 h, the sample is calcined at

---

* Corresponding author. Tel.: +86 22 23500876; fax: +86 22 23500876.
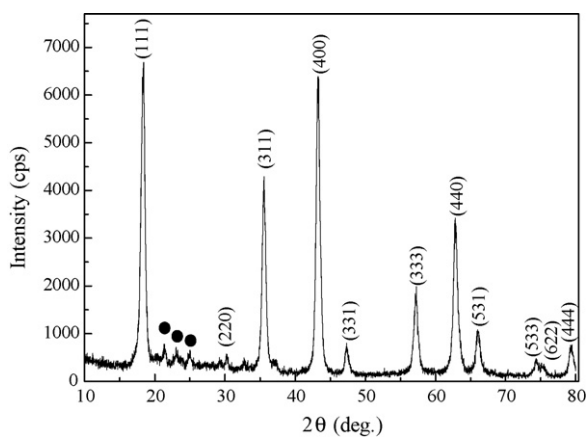*E-mail address:* xpgao@nankai.edu.cn (X.P. Gao).

Fig. 1. XRD pattern of as-prepared $Li_4Ti_5O_{12}$. A trace of TiO_2 phase can be detected as indicated by solid circle.

500 °C for 2 h with a rate of 2 °C min^{-1} in muffle furnace under Ar atmosphere. The as-prepared sample was characterized by X-ray diffraction (XRD, RIGAKU D/max-2500), scanning electron microscopy (SEM, HITACHI S-4800), and transmission electron microscopy (TEM, FEI Tecnai 20).

2.2. Electrochemical measurements

The working electrode was prepared by compressing a mixture of active materials, acetylene black, and binder (poly(tetrafluoroethylene), PTFE) in a weight ratio of 80:15:5. Lithium metal was used as the counter and reference electrodes. The electrolyte was $LiPF_6$ (1 M) dissolved in a mixture of ethylene carbonate (EC), ethyl methyl carbonate (EMC) and dimethyl carbonate (DMC) with a volume ratio of 1:1:1. The galvanostatic method at the charge/discharge current densities of 200, 500, 1000, 1500 and 2000 mA g^{-1} was employed to measure the electrochemical capacity and cycle life of working electrodes at room temperature using a LAND-CT2001A instrument. The cut-off potentials for charge and discharge were set at 2.5 and 1.0 V (vs. Li/Li$^+$), respectively. The cyclic voltammetry experiment was conducted using a CHI 600A potentiostat at a scan rate of 0.1, 0.5, 1, 2 and 4 mV s^{-1}, respectively.

3. Results and discussion

After calcination at 500 °C, crystalline spinel $Li_4Ti_5O_{12}$ (JCPDS 49-207) with a trace of TiO_2 phase can be detected as shown in the XRD pattern (Fig. 1). The crystallite size of $Li_4Ti_5O_{12}$, calculated by Scherrer's formula, is about 12.5 nm. The representative

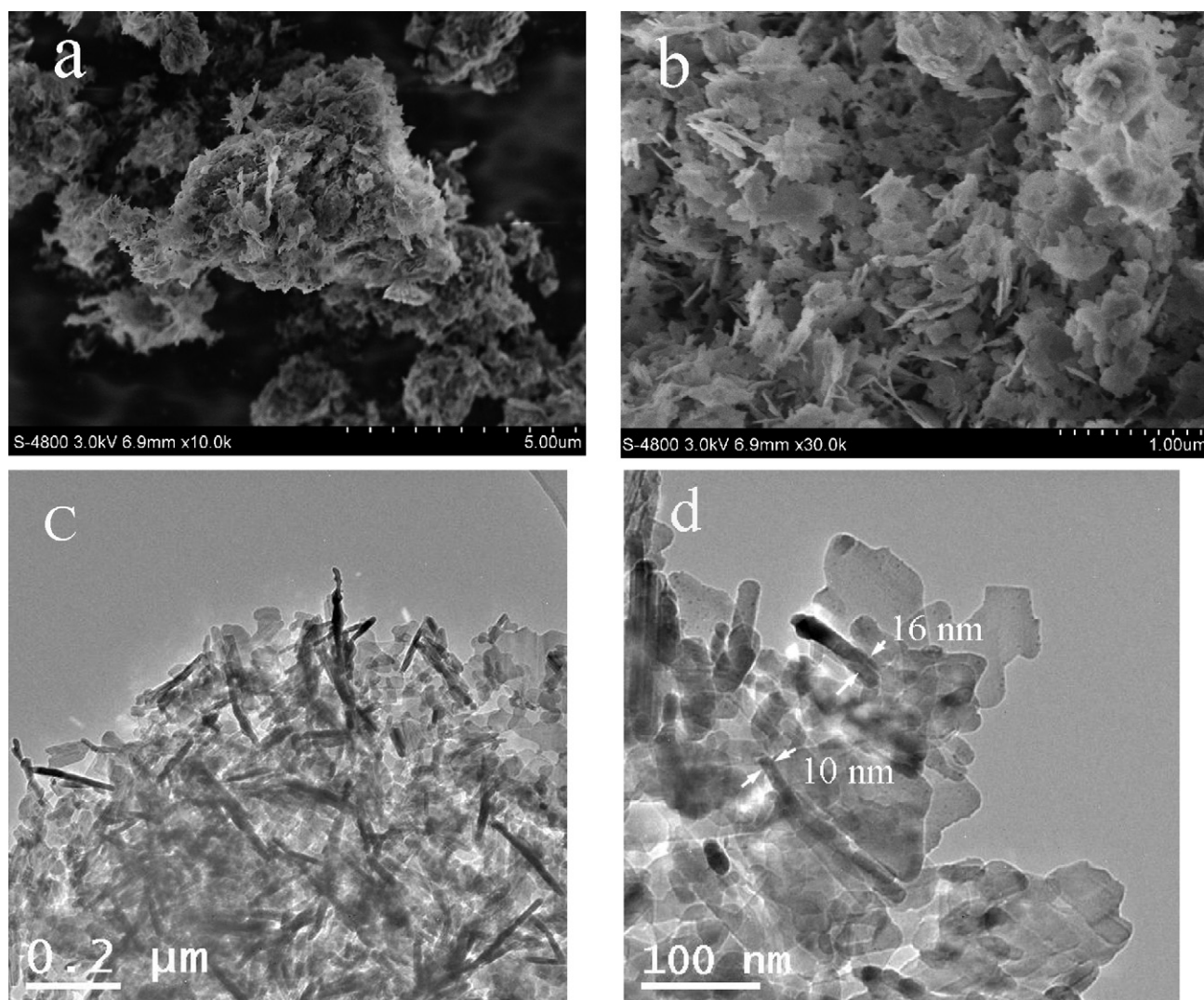**Fig. 2.** SEM (a and b) and TEM (c and d) images of the as-prepared $Li_4Ti_5O_{12}$.

SEM and TEM images are given in Fig. 2. From the SEM images, it is shown that the as-prepared sample is micro-sized agglomerates consisting of random sheet-like $Li_4Ti_5O_{12}$. The randomly oriented $Li_4Ti_5O_{12}$ with the perpendicular and parallel nanosheets can be clearly observed as shown in TEM images (Fig. 2c). The thickness of $Li_4Ti_5O_{12}$ nanosheets is about 10–16 nm by approximately calculating from the relative dark and rod-like edge shown by arrows in Fig. 2d. Combining all the results, it can be concluded that nanocrystalline $Li_4Ti_5O_{12}$ with a hierarchical structure is successfully prepared via the hydrothermal process and following calcination.

In order to show the cycle stability and high rate discharge ability, the variation in discharge capacity with cycles for the as-prepared $Li_4Ti_5O_{12}$ electrode at different current densities from 200 to 2000 mA g^{-1} are depicted in Fig. 3a. The discharge capacity of about 147.3 mAh g^{-1} is obtained after 10th cycle at the current density of 200 mA g^{-1}, and this value is lowered to 142.4, 138.3, 133.7 and 128 mAh g^{-1} at the current densities of 500, 1000, 1500 and 2000 mA g^{-1}, respectively. The capacity retention is about 87% at the high current density of 2000 mA g^{-1} (11.4 C) as compared to that at the low current density of 200 mA g^{-1} (1.1 C), indicating that the as-prepared sample can endure great changes of various discharge current densities to retain a good stability upon cycling.

The galvanostatic discharge/charge curves of the as-prepared samples at different current density corresponding to different cycle are presented in Fig. 3b. At the current density of 200 mA g^{-1}, the discharge/charge curves display a pair of flat potential plateaus around 1.53 and 1.6 V (vs. Li/Li$^+$), well corresponding to the two-phase equilibrium between $Li_4Ti_5O_{12}$ and $Li_7Ti_5O_{12}$ [7,9]. Upon increasing the current density, the flat potential plateau is maintained, even at the current density of 2000 mA g^{-1}. The small potential polarization of as-prepared sample indicates good reaction kinetics, consistent with the excellent high rate capability and nanosheet structure.

To better understand the high rate discharge nature of the as-prepared sample, cyclic voltammetry experiment at different scan rates was conducted as given in Fig. 4. After the initial two cycles, there is only a pair of sharp redox peaks appearing around 1.48 and 1.67 V (vs. Li/Li$^+$) at a low scan rate of 0.1 mV s^{-1}, corresponding to
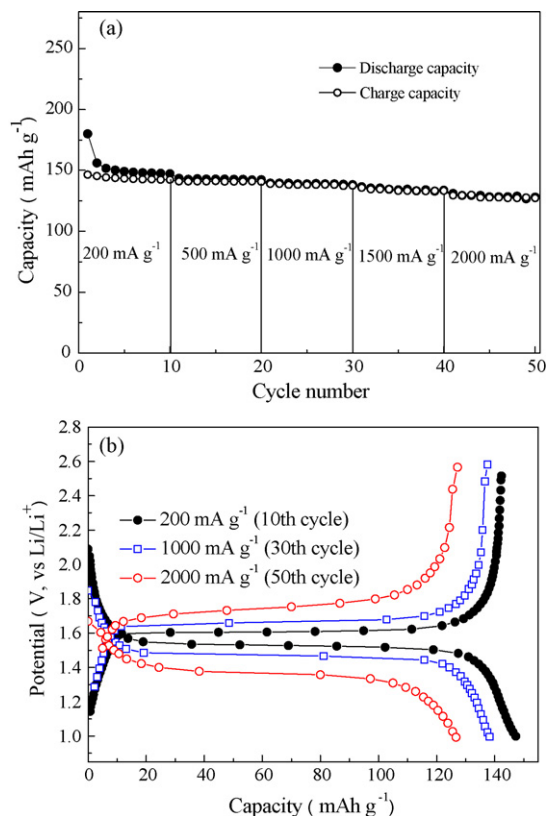

Fig. 3. Cycle performance of the as-prepared $Li_4Ti_5O_{12}$ at different current density in the potential ranging from 1.0 to 2.5 V (a) and discharge/charge curves of the as-prepared $Li_4Ti_5O_{12}$ at the different current density (b).

the insertion and extraction process of lithium ions in the spinel $Li_4Ti_5O_{12}$ [17–20]. While, a pair of redox peaks of 1.76 and 1.95 V (vs. Li/Li$^+$) at a low scan rate of 0.1 mV s^{-1} is not detected [12], indicating the effect of a trace of anatase TiO_2 in the as-prepared sample can be negligible. In particular, different from previous reports
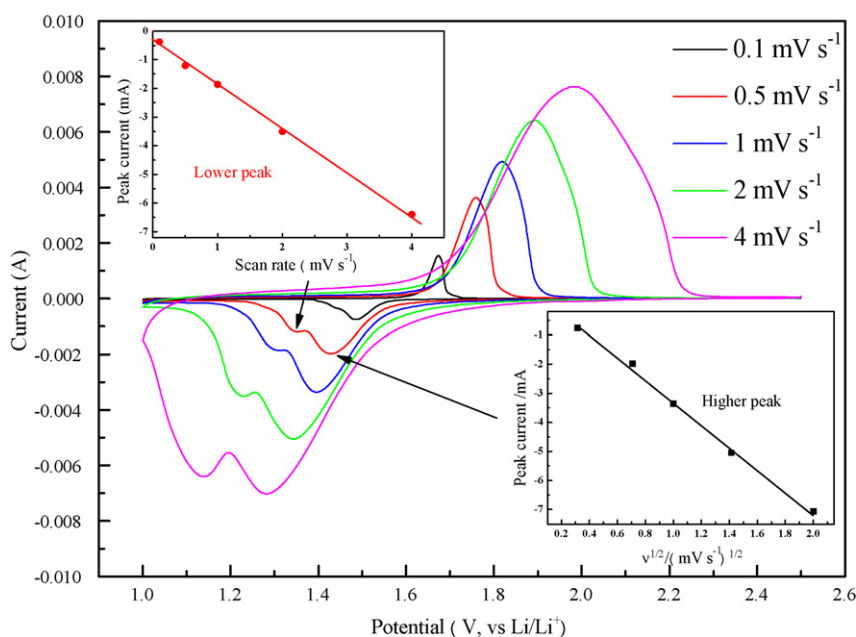

Fig. 4. Cyclic voltammograms of the as-prepared $Li_4Ti_5O_{12}$ at different scan rates after initial three cycles at a scan rate of 0.1 mV s^{-1}. The relationships between the peak current and scan rate in the cathodic process are inserted into this figure.

[17–21], two peaks can be clearly shown in the cathodic process of the hierarchical $Li_4Ti_5O_{12}$ at high scan rates (over 0.1 mV s^{-1}). It is well known that the relation between peak currents and scan rates indicates the different electrochemical reaction characteristics, including solid phase diffusion-controlled or surface-confined charge-transfer processes. The dependence of the peak current on the square root of the scan rate indicates an obvious diffusion-limited reaction for the higher peak (1.48, vs. Li/Li$^+$ at 0.1 mV s^{-1}) in the cathodic process for the as-prepared spinel $Li_4Ti_5O_{12}$. On the contrary, the pseudocapacitive effect can be confirmed by measuring the linear relationship between the peak current and the scan rate (ν) [12–14]. The lower peak (1.34 V, vs. Li/Li$^+$ at 0.5 mV s^{-1}) in the cathodic process can be designated as the surface lithium storage process corresponding to the faradaic reaction [15]. Obviously, the pseudocapacitive character is presented according to the linear relationship between the peak current and scan rate for the lower peak in the cathodic process as inserted in Fig. 4.

As mentioned above, faradic pseudocapacitive effect, taking place on the surface of nanosheets [13,14], is favorable to enhance the high rate discharge performance of electrode materials [15,16], which can give a powerful explanation of the superior electrochemical performance of as-prepared sample. It means that a mixed process of the faradaic pseudocapacitive and diffusion-limited reaction can be obtained for the hierarchical structured $Li_4Ti_5O_{12}$ with smaller grain sizes and short Li-transport lengths, instead of only solid diffusion-limited reaction in bulk materials. By considering all the results, the unique hierarchical structure, smaller grain sizes, and the resulting pseudocapacitive contribution of as-prepared $Li_4Ti_5O_{12}$ are considered as the main reason for the excellent high rate capability and good capacity retention at high current densities.

4. Conclusions

In conclusion, hierarchical structured $Li_4Ti_5O_{12}$ consisting with randomly oriented nanosheets was prepared via a facile hydrothermal route and following calcinations. The obvious pseudocapacitive characteristic can be clearly observed for the as-prepared $Li_4Ti_5O_{12}$ electrode by analyzing cyclic voltammograms, which is mainly related to an interfacial charge transfer and storage process, and hence can enhance the high rate capability of $Li_4Ti_5O_{12}$ nanosheets. Combining its unique structure and pseudocapacitive characteristic, the as-prepared sample presents the excellent cycle performance and good capacity retention at high current densities, which are among most important electrochemical performance in the application of electrode-active materials and batteries.

References

[1] M. Armand, J.M. Tarascon, Nature 451 (2008) 652.
[2] A. Manthiram, A.V. Murugan, A. Sarkar, T. Muraliganth, Energy Environ. Sci. 1 (2008) 621.
[3] Y. Li, G.L. Pan, J.W. Liu, X.P. Gao, J. Electrochem. Soc. 156 (2009) A495.
[4] J.J. Huang, Z.Y. Jiang, Electrochim. Acta 53 (2008) 7756.
[5] Y.F. Tang, L. Yang, S.H. Fang, Z. Qiu, Electrochim. Acta 54 (2009) 6244.
[6] E.M. Sorensen, S.J. Barry, H.K. Jung, J.M. Rondinelli, J.T. Vaughey, K.R. Poeppelmeier, Chem. Mater. 18 (2006) 482.
[7] K.S. Park, A. Benayad, D.J. Kang, S.G. Doo, J. Am. Chem. Soc. 130 (2008) 14930.
[8] L. Cheng, X.L. Li, H.J. Liu, H.M. Xiong, P.W. Zhang, Y.Y. Xia, J. Electrochem. Soc. 154 (2007) A692.
[9] Y.G. Wang, H.M. Liu, K.X. Wang, H. Eiji, Y.R. Wang, H.S. Zhou, J. Mater. Chem. 19 (2009) 6789.
[10] J. Kim, J. Cho, Electrochem. Solid-State Lett. 10 (2007) A81.
[11] A.S. Arico, P. Bruce, B. Scrosati, J.M. Tarascon, W.V. Schalkwijk, Nat. Mater. 4 (2005) 366.
[12] H. Zhang, G.R. Li, L.P. An, T.Y. Yan, X.P. Gao, H.Y. Zhu, J. Phys. Chem. C 111 (2007) 6143.
[13] J.R. Li, Z.L. Tang, Z.T. Zhang, Chem. Phys. Lett. 418 (2006) 506.
[14] L. Kavan, M. Kalbac, M. Zukalova, I. Exnar, V. Lorenzen, R. Nesper, M. Graetzel, Chem. Mater. 16 (2004) 477.
[15] J. Wang, J. Polleux, J. Lim, B. Dunn, J. Phys. Chem. C 111 (2007) 14925.
[16] P. Balaya, Energy Environ. Sci. 1 (2008) 645.
[17] Y.F. Tang, L. Yang, Z. Qiu, J.S. Huang, Electrochem. Commun. 10 (2008) 1513.
[18] C.H. Jiang, E. Hosono, M. Ichihara, I. Honma, H.S. Zhou, J. Electrochem. Soc. 155 (2008) A553.
[19] S. Bach, J.P. Pereira-Ramos, N. Baffier, J. Power Sources 81–82 (1999) 273.
[20] J.R. Li, Z.L. Tang, Z.T. Zhang, Electrochem. Commun. 7 (2005) 894.
[21] J.Q. Deng, Z.G. Lu, I. Belharouak, K. Amine, C.Y. Chung, J. Power Sources 193 (2009) 816.